Cell Biology International ISSN 1065-6995
doi: 10.1002/cbin.10388

RESEARCH ARTICLE

Knockdown of tumor protein D52-like 2 induces cell growth inhibition and apoptosis in oral squamous cell carcinoma

Yongchun He, Fengshan Chen*, Ying Cai and Sihui Chen

Department of Orthodontics, Laboratory of Oral Biomedical Science and Translational Medicine, School of Stomatology, Tongji University, Shanghai 200072, P. R. China

Abstract

Tumor protein D52-like 2 (TPD52L2) and its family members form homo- and hetero-meric complexes essential for cell proliferation in multiple human cancers. TPD52L2 is involved in cell migration and attachment in oral squamous cell carcinoma (OSCC). To confirm the role of TPD52L2 in OSCC, we employed the lentivirus-delivered small interfering RNA (siRNA) technique to knock down TPD52L2 expression in two OSCC cell lines, CAL27, and KB. Knockdown of TPD52L2 by RNA interference markedly suppressed cell proliferation and colony formation. Cell cycle analysis showed that depletion of TPD52L2 led to CAL27 cells arrest in the S phase. We found an excessive accumulation of cells in the sub-G1 phase, which can represent apoptotic cells. TPD52L2 silencing also induced the cleavage of PARP. These results suggest that TPD52L2 is involved in OSCC cell growth and serves as a potential therapeutic target in human OSCC.

Keywords: apoptosis; growth; oral squamous cell carcinoma; TPD52L2

Introduction

Oral squamous cell carcinoma (OSCC) is the most common oral malignancy, representing up to 80–90% of all malignant neoplasms of the oral cavity. Although oral cavity ranges from the 6–9th most common anatomical location for human cancer, it represents the most common location for cancer in specific countries, especially in southeastern Asia (Johnson et al., 2011). In Southeastern Asia, the disease is reaching epidemic proportions with age-standardized rates (ASR) of 6.7 compared to 4.3 and 4.0 in Europe and America, respectively (Ferlay et al., 2010). OSCC is susceptible to any site of oral mucosa and more prevalent among males with variable male:female ratio ranging from 6:1–2:1 (Gervasio et al., 2001; Al-Rawi and Talabani, 2008; Losi-Guembarovski et al., 2009; Grimm, 2012). However, several other recent studies have shown an increase in the number of affected females, with a mean male:female ratio lower than 2:1, probably due to changes in social and daily activities associated to modern women social profile and way of living, leading to higher exposure to carcinogenic agents (Andisheh-Tadbir et al., 2008; Gaitan-Cepeda et al., 2011; Kruse et al., 2011). OSCC has a survival rate of ~50% over 5 years, but this has not improved for decades, prompting the need to develop novel therapeutic therapies for treatments.

Cancer occurs due to accumulation of abnormalities in cellular DNA which, in turn provide a selective growth advantage to cancer cells and facilitate metastatic dissemination (Vogelstein and Kinzler, 2004). Thus, gene dysregulation is a critical factor for carcinogenesis and tumor progression. Tumor protein D52-like 2 (TPD52L2 or D54) is a member of the tumor protein D52-like family, which is also comprised of TPD52 (D52), TPD52L1 (D53), and TPD52L3 (D55). These proteins are characterized by an N-terminal coiled-coil motif that is used to form homo- and hetero-meric complexes with other tumor protein D52-like proteins. To date, TPD52 family members are emerging as important factors in tumor growth. TPD52 was originally identified by its elevated expression in human breast carcinoma (Byrne et al., 1998). Likewise, TPD52L1 was reported to be a cell cycle-regulated protein maximally expressed in G2-M transition and thus mediated breast

*Corresponding author: e-mail: fengshandr@163.com
Yongchun He and Fengshan Chen contributed to this work equally.
Abbreviations: TPD52L2, tumor protein D52-like 2; OSCC, oral squamous cell carcinoma; RNAi, RNA interference; shRNA, short hairpin RNA; siRNA, small interfering RNA

cancer cell growth (Boutros and Byrne, 2005). In testicular germ cell tumors, TPD52 is exclusively expressed in seminomas and embryonal carcinomas, but is absent in normal germ cells and most intratubular germ cell neoplasias (Alagaratnam et al., 2009). Additionally, altered expression of TPD52 regulated apoptosis and migration of prostate cancer cells (Ummanni et al., 2008). TPD52L3 was also observed to interact with other TPD52 family members and involved in testis development (Cao et al., 2006). RT-PCR analysis showed that TPD52 and TPD52L2 transcripts were frequently detected in acute lymphoblastic leukemia (ALL) and acute myeloid leukemia (AML), where they were frequently co-expressed (Barbaric et al., 2006). Interaction of TPD52L2 with hABCF3, a human non-transmembrane ATP-binding cassette protein, enhances the proliferation of liver cancer cell lines in vitro; disruption of this interaction significantly decreases cell growth (Zhou et al., 2013). Thus, it could be concluded that tumor protein D52-like family members are widely involved in human cancers with homo- and hetero-meric interactions.

The role of TPD52L2 in human oral cancers has only recently emerged. Mukudai et al. (2013) identified TPD52L2 as a negative regulator of extracellular matrix-dependent migration and attachment in OSCC-derived cell lines. To confirm the role of TPD52L2 in OSCC, we examined the effects of TPD52L2 on cell growth via lentivirus-delivered small interfering RNA (siRNA) in two OSCC cell lines, CAL27 and KB. Functional analyses were subsequently conducted by MTT, colony formation, flow cytometry and Western blot assays.

Materials and methods

Cell lines and cell culture

Human OSCC cell line CAL27 was bought from American Tissue Culture Collection (ATCC). Human OSCC cell line KB was obtained from Cell Bank of Chinese Academy of Science (Shanghai, China). Cells were maintained in Dulbecco's Modified Eagle Medium (DMEM, Hyclone, Logan, UT) supplemented with 10% heat-inactivated fetal bovine serum (FBS) at 37°C in humidified atmosphere of 5% CO_2.

Reagents

Goat anti-TPD52L2 was purchased from Sigma (#SAB2501053, St. Louis, MO). Rabbit anti-PARP was purchased from Cell Signaling Technology (#9542, Danvers, MA). Rabbit anti-GAPDH was commercially from Proteintech Group, Inc. (#10494-1-AP, Chicago, IL). Donkey anti-goat secondary antibody was from Beyotime Institute of Biotechnology (#A0181, Nantong, China), and goat anti-rabbit secondary antibody was from Santa Cruz (#SC-2054, CA).

Construction of TPD52L2 shRNA-expressing lentivirus

Small interfering RNAs (siRNA) were transformed into short hairpin RNA (shRNA) (stem-loop-stem structure). The shRNA sequence (5′-GCGGAGGGTTTGAAAGAA-TATCTCGAGATATTCTTTCAAACCCTCCGCTTTTTT-3′) targeting TPD52L2 (NM_199360) was inserted into the pFH-L plasmid (Shanghai Hollybio, China). A scrambled shRNA that shared no homology with the mammalian genome(5′-CTAGCCCGGCCAAGGAAGTGCAATTGCA-TACTCGAGTATGCAATTGCACTTCCTTGGTTTTTTGT-TAAT-3′) was used as control. To rule out the possible off-target effect of shRNA, another shRNA sequence (5′-CTCTACAA-GAAGACTCAGGAACTCGAGTTCCTGAGTCTTCTTG-TAGAGTTTTTT-3′) against TPD52L2 was used to get comparable results. The lentivirus-based shRNA-expressing vectors were constructed, confirmed by DNA sequencing and termed pFH-L-shTPD52L2 or pFH-L-shCon. For transfection, HEK293T cells (6×10^4/well) were seeded in 6-well plates and cultured for 36 h to reach 90% confluence. At 2 h before transfection, the medium was replaced with serum-free medium. The plasmid mixture containing pFH-L-shTPD52L2 (or pFH-L-shCon) and pVSVG-I/pCMVΔR8.92 packaging vectors, as well as Lipofectamine 2000 (Invitrogen, Carlsbad, CA) were added to the cells. At 5 h after incubation, the medium was replaced with DMEM containing 10% FBS. Lentiviral particles (Lv-shTPD52L2 or Lv-shCon) were harvested at 72 h after transfection and purified by ultra-centrifugation. CAL27 and KB cells were then transduced with lentiviral particles at a multiplicity of infection (MOI) of 15, respectively.

Quantitative real-time PCR (qRT-PCR)

Total RNA of cultured cells were extracted using Trizol solution (Invitrogen) at 24 h post-transfection. Equal amounts of RNA (2000 ng) were reverse-transcribed into cDNA using the PrimeScript RT Master Mix Perfect Real Time (TaKaRa, Shiga, Japan). qRT-PCR was subsequently performed in an ABI PRISM 7900 Real-Time System. Ten-fold dilution of each cDNA was amplified in a 50 μL volume, using the SYBR Premix Ex Taq™ Perfect Real Time (TaKaRa).

Actin was used as interference control. Primers used were as follows:

TPD52L2, Forward 5′-TTCACAGGCAGGACAGAAGA-3′
Reverse 5′- TTGAAGGTCGCAGAGTTCCT-3′
Actin, Forward 5′-GTGGACATCCGCAAAGAC-3′
Reverse 5′- AAAGGGTGTAACGCAACTA-3′

Primers were synthesized by Shanghai Daweike Biotechnology Co. Ltd (Shanghai, China). PCR cycle conditions were 95°C for 30 s, and 40 cycles of 95°C for 5 s, and 60°C for 34 s. The amplification specificity was evaluated with melting curve analysis. Relative mRNA was determined by using the

formula $2^{-\Delta CT}$ (CT, cycle threshold) where $\Delta CT = CT$ (target gene) − CT (Actin). Each experiment was performed in triplicate and repeated three times.

Western blot analysis

Protein concentration was determined first by using the Bio-Rad DC Protein Assay (Bio-Rad, CA). Equal amount of protein (30 μg) was loaded into each well and subjected to one-dimensional SDS-polyacrylamide gel. Subsequently, proteins were transferred to a polyvinylidene difluoride membrane using a transfer apparatus according to manufacturer's instructions (Bio-Rad). Membranes were blocked with 5% nonfat dry milk in TBST buffer (10 mM Tris–HCl, pH8.0, and 150 mMNaCl) containing 0.05% Tween-20. Thereafter, membranes were probed with anti-TPD52L2, anti-PARP, or anti-GAPDH antibody at 4°C overnight. The secondary antibody, donkey anti-goat or goat anti-rabbit immunoglobulin G linked with horse radish peroxidase, was added in the presence of the blocking agent and incubated with membranes for 2 h at room temperature. Immunoreactivity was detected with enhanced chemoluminescent autoradiography (ECL kit, Amersham). Each experiment was repeated three times.

MTT cell viability assay

For viability, 3-(4,5-dimethylthiazol-2-yl)-2,5-diphenyltetrazolium bromide (MTT) colorimetric assay was used. Briefly, after lentivirus infection, CAL27 and KB cells were washed with PBS and suspended at a final concentration of 2×10^3 cells/well in an assay medium and dispensed into 96-well plates. The plates were incubated at 37°C for 5 days in a humidified air + CO_2 incubator. At each time-point (1, 2, 3, 4, and 5 days), 100 ml MTT (5 mg/mL) was added to each well, the plates were incubated at 37°C for 4 h, and 100 μL acidic isopropanol (10% SDS, 5% isopropanol, and 0.01 mol/L HCl) was added to each well. The absorbance at 595 nm was measured using a synergy 2 multi-mode microplate reader (Bio Tek Instruments, Winooski, VT). Each experiment was performed in triplicate and repeated three times.

Plate colony formation assay

CAL27 cells (500 cells/well) were seeded into 6-well plates 4 days after lentivirus infection. The medium was changed at 2-day intervals. After 6 days of culture at 37°C, cells were washed with PBS and fixed with 4% paraformaldehyde for 30 min at room temperature. The fixed cells were stained with freshly prepared Crystals purple (Merck) for 10 min, washed with water and air-dried. The total number of colonies with >50 cells was counted with a light microscope and a fluorescent microscope. Each experiment was done in triplicate and repeated three times.

FACS analysis

Flow cytometry was used to assess whether CAL27 cells were arrested at a particular stage of the cell cycle. CAL27 cells (2×10^5 cells/dish) were seeded into 6 cm dishes and inoculated with recombined lentivirus at an MOI of 10 for 3 days. Cells were collected by centrifugation at 1500 rpm for 5 min, washed with ice-cold PBS, and suspended in about 0.5 mL of 70% cold alcohol. The fixed cells were resuspended in propidium iodide (PI)/RNase/PBS buffer for incubation in dark (37°C, 30 min), and stained cells were analyzed with a FACs caliber II sorter and Cell Quest FACS system (BD Biosciences, San Diego, CA). The percentage of cells in each cell cycle phase was assessed. Each experiment was performed in triplicate and repeated three times.

Statistical analysis

Data were presented as mean ± SD of three independent experiments. The Student's *t*-test was used to calculate the differences, and $P < 0.05$ was considered statistically significant.

Results

Specific knockdown of TPD52L2 by RNA interference in CAL27 cells

Generally, the siRNA targeting is effective over a short period, and the gene transcription will return to normal after 3–7 days (McManus and Sharp, 2002). Lentivirus-based vectors have been successfully used for gene targeting to deliver siRNA with long-term silencing efficiency (Devi, 2006). Therefore, we examined the biological role of TPD52L2 via lentivirus-mediated siRNA in two OSCC cell lines. Approximately 90% cells were successfully transduced with lentivirus particles, as evidenced by the GFP signals (Figure 1A). The expression of TPD52L2 mRNA was analyzed in CAL27 cells by qRT-PCR. The relative expression of TPD52L2 was significantly decreased after Lv-shTPD52L2 infection by a 92.4% reduction in CAL27 cells (Figure 1B, $P < 0.01$). The efficiency of knockdown was satisfying, and western blot confirmed the silencing of TPD52L2 protein. Marked suppression of TPD52L2 was observed in CAL27 cells infected with Lv-shTPD52L2 (Figure 1C). Similarly, another Lv-shTPD52L2 (Lv-shTPD52L2 #2) also efficiently transduced into both CAL27 and KB cells (see Supporting Information, Figure S1A and B). The protein levels of TPD52L2 were significantly decreased in Lv-shTPD52L2 #2 infected cells (Figure S1C and D). Our constructed Lv-shTPD52L2 could efficiently and

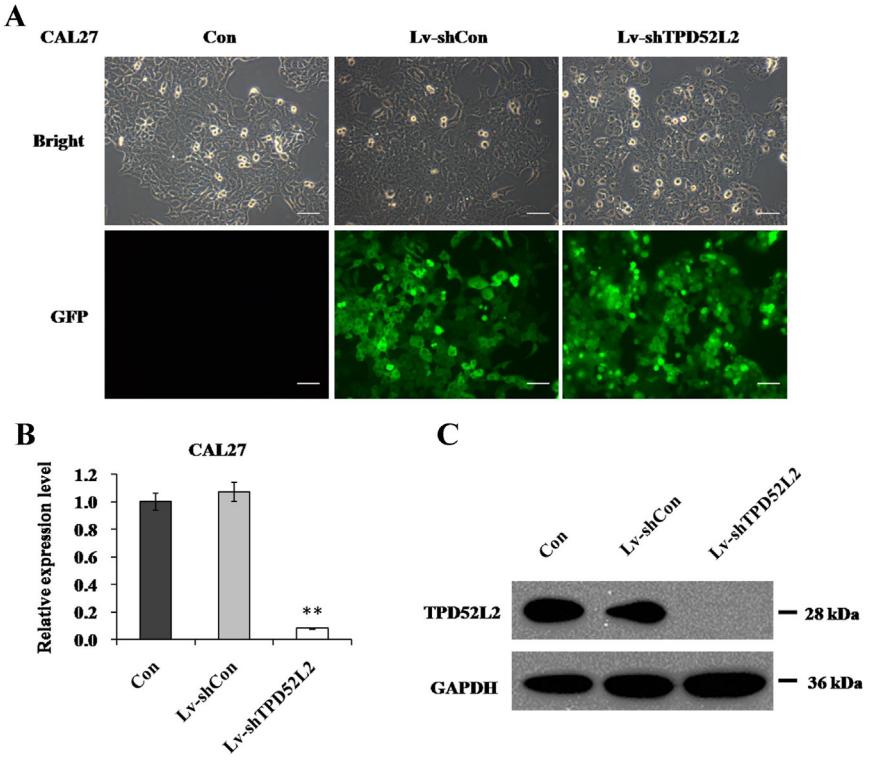

Figure 1 Specific knockdown of TPD52L2 by Lv-shTPD52L2 in CAL27 cells. (A) Representative graphs of lentivirus infection efficiency were shown. CAL27 cells were infected with Lv-shTPD52L2 at an MOI of 15 (magnification ×100). (B) qRT-PCR analysis of the knockdown efficiency of Lv-shTPD52L2 in CAL27 cells. Actin was used as a negative control. (C) Western blot analysis of the knockdown efficiency of Lv-shTPD52L2 in CAL27 cells. GAPDH was used as a control. $^{**}P < 0.01$, Lv-shTPD52L2 group versus Lv-shCon group. Scale bar: 50 μm.

specifically knock down endogenous TPD52L2 expression in CAL27 and KB cells.

Knockdown of TPD52L2 inhibits cell proliferation and colony formation in vitro

To investigate the effects of TPD52L2 on cell proliferation in vitro, MTT assay was used to monitor the proliferation rate of CAL27 cells daily for 5 days. Viable cell numbers in the Lv-shTPD52L2 group were different from those in Lv-shCon group or control group on day 2 (Figure 2A). On day 4, cell proliferation was strongly inhibited in CAL27 cells after TPD52L2 knockdown ($P < 0.001$). By day 5, viable cell numbers in the Lv-shTPD52L2 group were only 22.3% those in the Lv-shCon group ($P < 0.001$). There was no significant difference in the proliferation between Lv-shCon infected cells and control cells. Similarly, the proliferative ability was markedly impaired in CAL27 and KB cells after Lv-shTPD52L2 #2 infection, respectively ($P < 0.001$, Figure S1E and F).

Colony formation assay was used to measure the tumorigenesis ability in vitro. Both the number of colonies and the size of single colony formed in CAL27 cells were obviously decreased in the Lv-shTPD52L2 group compared with control groups (Figure 2B). Approximately 10 colonies were observed in bright field or with the help of Cristal violet staining, as well as fluorescent presentation. However, ~350 colonies were seen in the Lv-shCon group or control group. Exact counting of colony numbers showed the number of colonies was significantly reduced in Lv-shTPD52L2 infected cells (Figure 2C, $P < 0.001$). These results indicate that the shRNA-mediated knockdown of TPD52L2 resulted in a significant inhibition in CAL27 cell growth in vitro.

Knockdown of TPD52L2 induces S phase arrest and apoptosis

In breast cancer, TPD52L1 was reported to mediate breast cancer cell growth as a cell cycle-regulated protein. Since D52-like protein sequences are all predicted to contain a coiled-coil domain which is essential for protein interaction (Byrne and Nourse, 1998), we hypothesized that the growth suppression of CAL27 cells by the shRNA-mediated TPD52L2 silencing was caused by disruption of cell cycle transition with delay in mitotic entry, which has been shown

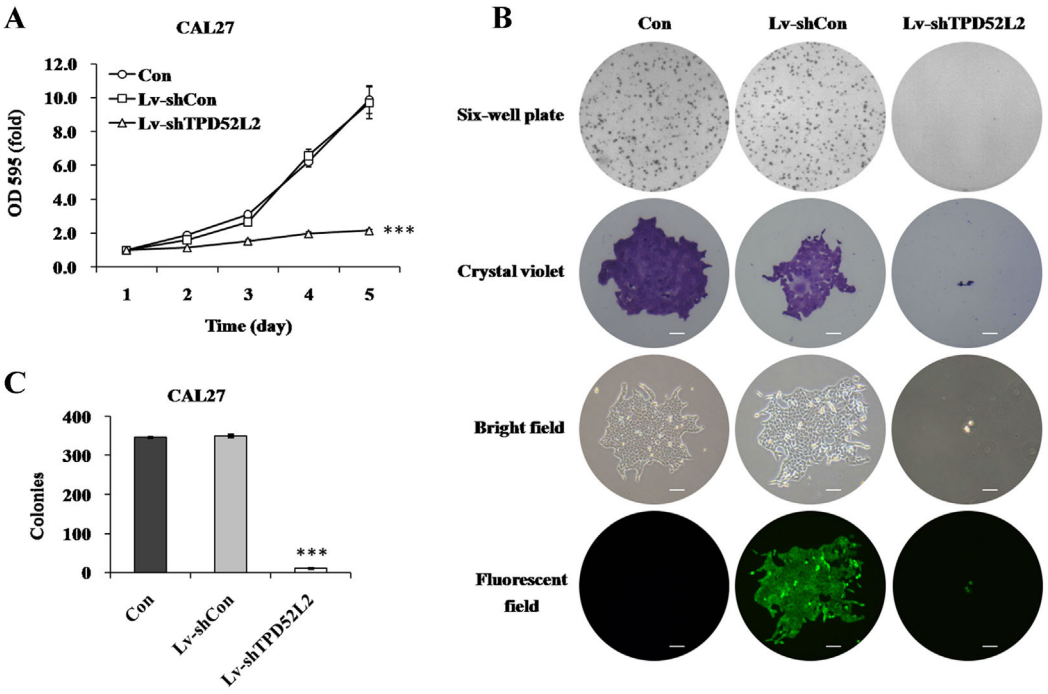

Figure 2 Knockdown of TPD52L2 inhibits the proliferation and colony formation of CAL27 cells. (A) Cell proliferative rate was significantly slowed down in Lv-shTPD52L2 infected cells compared with Lv-shCon infected cells, as measured by MTT assay. (B) Colony formation assay was performed to mimic cell growth in vivo. Representative graphs of total colonies formed in CAL27 cells with three treatments in each well under light microscopy (upper one line). Representative graphs of a single colony formed in CAL27 cells with three treatments (lower three lines) using crystal violet staining (top), in bright field (middle), and fluorescence microscopy (bottom) (magnification ×40). Colonies were markedly less in the Lv-shTPD52L2 group than in control groups. (C) Colonies counting revealed that average colony numbers were significantly reduced after Lv-shTPD52L2 infection. ***$P < 0.001$, Lv-shTPD52L2 group versus Lv-shCon group. Scale bar: 125 μm.

in TPD52L1. To determine this, we analyzed the DNA contents of cell populations reflecting the cell cycle distribution in CAL27 cells after TPD52L2 depletion (Figure 3A). An increase in the S phase with a concomitant decrease in the G0/G1 phase was observed in CAL27 cells after Lv-shTPD52L2 infection (Figure 3B). Compared with an average 69.7% in G0/G1 stage of Lv-shCon infected cells, only 65.14% cells were distributed in G0/G1 stage of Lv-shTPD52L2 infected cells ($P < 0.01$). In turn, a significant increase in the S phase population (22.0%) of Lv-shTPD52L2 infected cells was observed as compared with only 17.7% cells distributed in the S phase of Lv-shCon infected cells ($P < 0.01$). In following the changes in the DNA content during the time course after infection, there was a notable increase in the sub-G1 populations 40 h post-infection in CAL27 cells. Approximate 1.2% cells were distributed at sub-G1 phase of Lv-shTPD52L2 infected cells, whereas only ∼0.1% cells in the sub-G1 phase in the Lv-shCon group or control group (Figure 3C, $P < 0.001$). These results indicate that knockdown of TPD52L2 in CAL27 cells led to an abnormal accumulation in the S phase, especially in the sub-G1 phase, which can represent apoptotic cells (Riccardi and Nicoletti, 2006). Alteration in the expression of an apoptosis marker, PARP, was detected in CAL27 cells. Depletion of TPD52L2 caused a significant increase in cleaved PARP expression (Figure 4), verifying the induction of apoptosis. These results suggest that knockdown of TPD52L2 in CAL27 cells could inhibit cell proliferation due to S phase cell cycle arrest and apoptosis.

Discussion

Oral squamous cell carcinoma (OSCC), a subset of head and neck squamous cell carcinoma (HNSCC), is one of the most common malignancies with >400,000 of new cases diagnosed annually worldwide (Jemal et al., 2011). Although OSCC is a disease of adults and elderly and its most common clinical aspect is an ulcerated lesion with necrotic central area surrounded by elevated rolled borders (Neville and Day, 2002). Nowadays it occurs gradually to those who are younger due to nutritional deficiencies and genetic changes. To date, mounting evidence has identified the key roles of D52-like proteins in tumor cell proliferation and apoptosis, making them proper for novel therapeutic target development. However, the association between D52-like proteins and OSCC growth was not fully understood, except for a

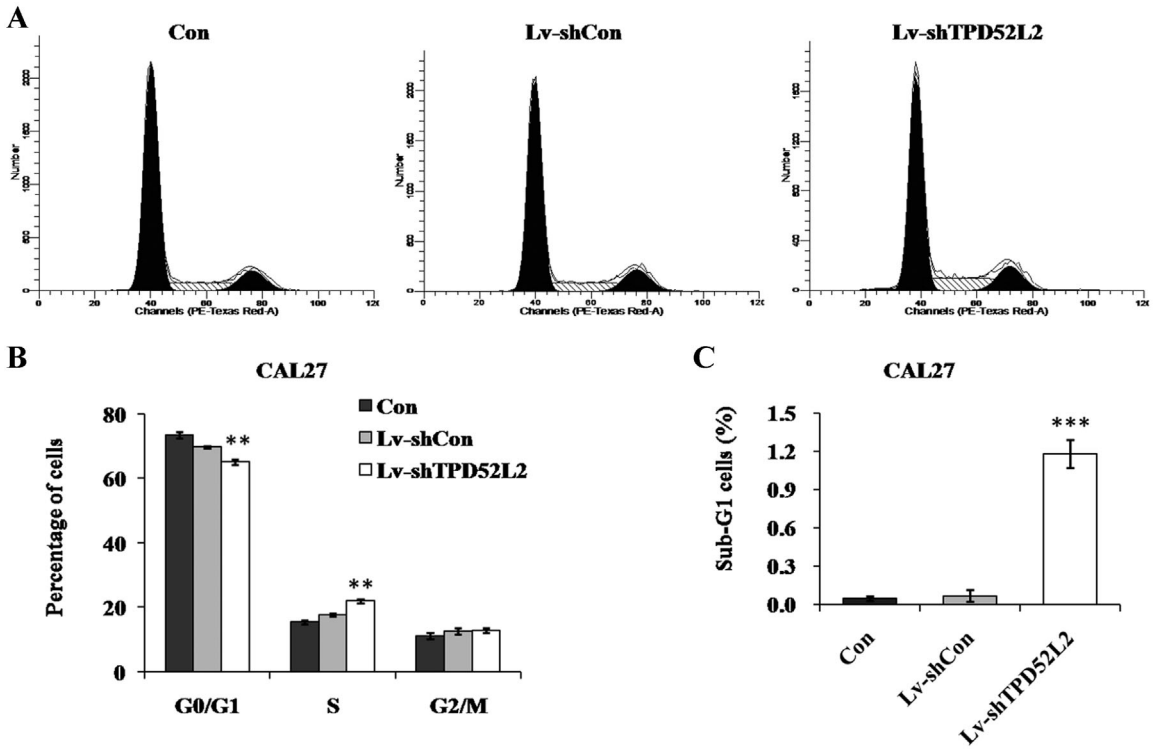

Figure 3 Knockdown of TPD52L2 induces S phase accumulation and apoptosis. (A) Cell cycle distribution was assessed to observe cell populations in distinct stages with FACS. The experiment was performed in triplicate and repeated three times. (B) Knockdown of TPD52L2 caused a significant increase in S phase population and decrease in the G0/G1 population. (C) Knockdown of TPD52L2 caused significant elevated sub-G1 population in CAL27 cells infected with Lv-shTPD52L2. $^{**}P < 0.01$, $^{***}P < 0.001$, Lv-shTPD52L2 group versus Lv-shCon group.

report of the negative role of TPD52L2 in OSCC cell migration and attachment (Mukudai et al., 2013). To determine whether the same results could be observed in another OSCC cell line, we employed an RNA interference lentivirus system to specifically knock down TPD52L2 expression in CAL27 and KB cells. The lentivirus infection efficiency was confirmed to be ~90%. Both the mRNA and protein levels of TPD52L2 were markedly decreased in Lv-shTPD52L2 infected cells.

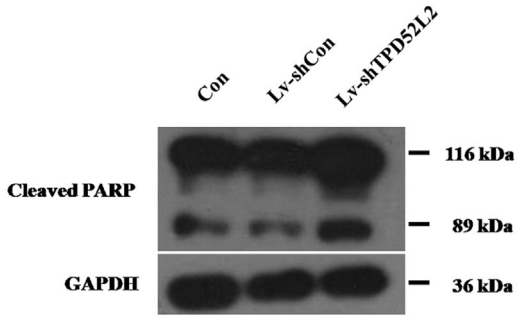

Figure 4 Knockdown of TPD52L2 induces the cleavage of PARP. Western blot analysis of PARP expression in CAL27 cells. GAPDH was used as control.

Cell viability assay reflects cell proliferative rate, which is a hallmark of cell numbers, and colony formation assay indicates the ability of cell growth in anchorage-independent condition, which is closely related to the in vivo situation (Wang, 2004). Our results indicate that knockdown of TPD52L2 remarkably suppressed the proliferation and colony formation of CAL27 cells, which was not supported by Mukudai et al. (2013); who showed that TDP52L2 did not contribute to proliferation of the OSCC cell line SAS. There appears to be context specificity as to whether TDP52L2 affects proliferation or not in different cell lines.

Subsequently, we explored whether the inhibition of proliferation was due to cell cycle arrest. Knockdown of TPD52L2 in CAL27 cells led to a significant increase in the S phase population with a concomitant decrease in the G0/G1 population. More importantly, depletion of TPD52L2 induced an excess accumulation of cells in the sub-G1 phase. Sub-G1 phase cells are usually considered to be the result of apoptotic DNA fragmentation: during apoptosis, the DNA is degraded by cellular endonucleases. Therefore, nuclei of apoptotic cells contain less

DNA than nuclei of healthy G0/G1 cells, resulting in a sub-G1 peak in the fluorescent histogram that may be used to determine the relative amount of apoptotic cells (Riccardi and Nicoletti, 2006). Depletion of TPD52L2 resulted in a significant increase in cleaved PARP expression, whose presence is one of the most frequently used diagnostic tools for the detection of apoptosis in many cell types (Bressenot et al., 2009). Overall, we speculate that knockdown of TPD52L2 might prevent cells passing the G2 checkpoint and thus lead to apoptosis. In cell cycle progression, a number of factors are involved to keep balance between activation and inactivation of CDKs should be achieved. It is conceivable that the regulatory mechanism by which TPD52L2 inhibits the proliferation of CAL27 cells might be related to the dysregulation of cyclins and CDKs. Cdc25 is an activating phosphatase that under favorable conditions removes the inhibitory phosphates present within the MPF (term for the cyclin B/CDK1 complex). Expression of TPD52L1 was paralleled to that of cyclin B (Boutros and Byrne, 2005). Therefore, the regulatory mechanism by which TPD52L2 inhibits cell proliferation might be related to dysregulation of Cdc25 and cyclin B/CDK1 complex, but more work on the regulation network will be needed.

Thus, knockdown of TPD52L2 inhibits the growth of CAL27 cells via inducing cell cycle arrest and apoptosis. We suggest that TPD52L2 as an essential molecule for OSCC growth and a potential target for halting proliferation and triggering apoptosis, which may provide novel clues for OSCC therapy.

Acknowledgments and funding

This work was supported by the National Natural Science Foundation of China (No. 81170942, 81371129) and the Natural Science Foundation of Shanghai (No. 10JC1415500).

References

Al-Rawi NH, Talabani NG (2008) Squamous cell carcinoma of the oral cavity: a case series analysis of clinical presentation and histological grading of 1,425 cases from Iraq. Clin Oral Investig 12: 15–8.

Alagaratnam S, Hardy JR, Lothe RA, Skotheim RI, Byrne JA (2009) TPD52, a candidate gene from genomic studies, is overexpressed in testicular germ cell tumours. Mol Cell Endocrinol 306: 75–80.

Andisheh-Tadbir A, Mehrabani D, Heydari ST (2008) Epidemiology of squamous cell carcinoma of the oral cavity in Iran. Journal Craniofac Surg 19: 1699–702.

Barbaric D, Byth K, Dalla-Pozza L, Byrne JA (2006) Expression of tumor protein D52-like genes in childhood leukemia at diagnosis: clinical and sample considerations. Leuk Res 30: 1355–63.

Boutros R, Byrne JA (2005) D53 (TPD52L1) is a cell cycle-regulated protein maximally expressed at the G2-M transition in breast cancer cells. Exp Cell Res 310: 152–65.

Bressenot A, Marchal S, Bezdetnaya L, Garrier J, Guillemin F, Plenat F (2009) Assessment of apoptosis by immunohistochemistry to active caspase-3, active caspase-7, or cleaved PARP in monolayer cells and spheroid and subcutaneous xenografts of human carcinoma. J Histochem Cytochem 57: 289–300.

Byrne JA, Nourse CR, Basset P, Gunning P (1998) Identification of homo- and heteromeric interactions between members of the breast carcinoma-associated D52 protein family using the yeast two-hybrid system. Oncogene 16: 873–81.

Cao Q, Chen J, Zhu L, Liu Y, Zhou Z, Sha J, Wang S, Li J (2006) A testis-specific and testis developmentally regulated tumor protein D52 (TPD52)-like protein TPD52L3/hD55 interacts with TPD52 family proteins. Biochem Biophys Res Commun 344: 798–806.

Devi G (2006) SiRNA-based approaches in cancer therapy. Cancer Gene Ther 13: 819–29.

Ferlay J, Shin HR, Bray F, Forman D, Mathers C, Parkin DM (2008) Estimates of worldwide burden of cancer in 2008: GLOBOCAN 2008. Int J Cancer 127: 2893–917.

Gaitan-Cepeda LA, Peniche-Becerra AG, Quezada-Rivera D (2011) Trends in frequency and prevalence of oral cancer and oral squamous cell carcinoma in Mexicans. A 20 years retrospective study. Med Oral Patol Oral Cir Bucal 16: e1–5.

Gervasio OL, Dutra RA, Tartaglia SM, Vasconcellos WA, Barbosa AA, Aguiar MC (2001) Oral squamous cell carcinoma: a retrospective study of 740 cases in a Brazilian population. Braz Dent J 12: 57–61.

Grimm M (2012) Prognostic value of clinicopathological parameters and outcome in 484 patients with oral squamous cell carcinoma: microvascular invasion (V +) is an independent prognostic factor for OSCC. Clin Transl Oncol 14: 870–8.

Jemal A, Bray F, Center MM, Ferlay J, Ward E, Forman D (2011) Global cancer statistics. CA Cancer J Clin 61: 69–90.

Johnson NW, Jayasekara P, Amarasinghe AA (2011) Squamous cell carcinoma and precursor lesions of the oral cavity: epidemiology and aetiology. Periodontol 2000 57: 19–37.

Kruse AL, Bredell M, Gratz KW (2011) Oral cancer in men and women: are there differences?. Oral Maxillofac Surg 15: 51–5.

Losi-Guembarovski R, Menezes RP, Poliseli F, Chaves VN, Kuasne H, Leichsenring A, Maciel ME, Guembarovski AL, Oliveira BW, Ramos G, Mizuno LT, Cavalli IJ, Ribeiro EM, Cólus IM (2009) Oral carcinoma epidemiology in Parana State, Southern Brazil. Cad Saude Publica 25: 393–400.

McManus MT, Sharp PA (2002) Gene silencing in mammals by small interfering RNAs. Nature Reviews Genetics 3: 737–4.

Mukudai Y, Kondo S, Fujita A, Yoshihama Y, Shirota T, Shintani S (2013) Tumor protein D54 is a negative regulator of extracellular matrix-dependent migration and attachment in oral squamous cell carcinoma-derived cell lines. Cell Oncol 36: 233–45.

Neville BW, Day TA (2002) Oral cancer and precancerous lesions. CA Cancer J Clin 52: 195–21.

Riccardi C, Nicoletti I (2006) Analysis of apoptosis by propidium iodide staining and flow cytometry. Nat Protoc 1: 1458–61.

Ummanni R, Teller S, Junker H, Zimmermann U, Venz S, Scharf C, Giebel J, Walther R (2008) Altered expression of tumor protein D52 regulates apoptosis and migration of prostate cancer cells. FEBS J 275: 5703–13.

Vogelstein B, Kinzler KW (2004) Cancer genes and the pathways they control. Nat Med 10: 789–99.

Wang LH (2004) Molecular signaling regulating anchorage-independent growth of cancer cells. Mt Sinai J Med 71: 361–7.

Zhou J, Lin Y, Shi H, Huo K, Li Y (2013) HABCF3, a TPD52L2 interacting partner, enhances the proliferation of human liver cancer cell lines in vitro. Mol Biol Rep 40: 5759–67.

Received 12 December 2013; accepted 31 July 2014.

Final version published online 13 October 2014.

Supporting Information

Additional supporting information may be found in the online version of this article at the publisher's web-site.

Figure S1. Specific knockdown of TPD52L2 by Lv-shTPD52L2 #2 in CAL27 and KB cells.